J Appl Physiol 108: 189–196, 2010.
First published October 1, 2009; doi:10.1152/japplphysiol.00669.2009.

Noninvasive real-time measurement of nasal mucociliary clearance in mice by pinhole gamma scintigraphy

Xiaoyang Hua,[1,2,6]* Kirby L. Zeman,[2]* Bingqing Zhou,[3] Qingquan Hua,[5] Brent A. Senior,[4] Stephen L. Tilley,[1,2] and William D. Bennett[1,2]

[1]*Pulmonary Division, Department of Medicine;* [2]*Center of Environmental Medicine, Asthma and Lung Biology;* [3]*Department of Biostatistics; and* [4]*Department of Otolaryngology, the University of North Carolina at Chapel Hill, Chapel Hill, North Carolina; and* [5]*Department of Otolaryngology, Ren-Ming Hospital, Wuhan University; and* [6]*Department of Otolaryngology, Tongji Hospital, Tongji Medical College, Huazhong University of Science and Technology, Wuhan, China*

Submitted 23 June 2009; accepted in final form 25 September 2009

Hua X, Zeman KL, Zhou B, Hua Q, Senior BA, Tilley SL, Bennett WD. Noninvasive real-time measurement of nasal mucociliary clearance in mice by pinhole gamma scintigraphy. *J Appl Physiol* 108: 189–196, 2010. First published October 1, 2009; doi:10.1152/japplphysiol.00669.2009.—Mucociliary clearance (MCC) is the key defense mechanism in the upper airways, as the removal of debris-laden mucus in the sinuses completely depends on MCC. So far, how the nasal MCC is regulated remains unknown. Recently, mice deficient in genes encoding the components of MCC apparatus have been generated, which will allow investigators to conduct more in-depth nasal MCC studies. However, the methodology necessary to comprehensively evaluate the nasal MCC in this species is not well established. We therefore developed a novel method to measure nasal MCC in live mice using pinhole gamma camera. Insoluble radiolabeled particles were delivered into the noses of lightly anesthetized mice. The nasal clearance of these particles was measured continuously in a real-time manner. The effect of three different anesthetics—avertin, pentobarbital, and isoflurane—on nasal MCC was also determined. In mice anesthetized by 1.1% isoflurane, radiolabeled particles were immediately moved into the oropharynx, which was significantly accelerated by the treatment of hypertonic but not isotonic saline. According to the clearance rate, the mouse nasal MCC presented two distinct phases: a rapid phase and a slow phase. In addition, we found that isoflurane had a very small inhibitory effect on nasal MCC vs. both avertin and pentobarbital. This was further supported by its dose response. Collectively, we have developed a noninvasive method to monitor the real-time nasal MCC in live mice under physiological conditions. It provides more comprehensive evaluation on nasal MCC rather than assessing a single component of the MCC apparatus in isolation.

anesthesia; isoflurane; avertin; pentobarbital; hypertonic saline

MUCOCILIARY CLEARANCE (MCC) is an important innate defense mechanism by which both upper and lower airways cleanse their surface of inhaled pollutants, allergens, pathogens, and mucus secreted by goblet cells and submucosal glands. This protective mechanism is especially important in the upper airways and sinuses, as the removal of debris-laden mucus in the sinuses completely depends on MCC, whereas in the lower airways MCC can be compensated for by other mechanisms such as coughing (43). This hypothesis is further supported by the observations that mice with primary ciliary dyskinesia (PCD) only exhibit inflammation in the nose and sinuses but not in the lower airways and lungs; and that sinonasal symptoms usually emerge in the early stage of PCD patients (6, 26, 28, 32, 45). These observations have led to the theory that impaired MCC in the nose and sinuses is the central pathophysiological process in the pathogenesis of chronic rhinosinusitis (CRS), a disease that currently affects more than 12% of Americans more than 18 years old (35). The major purpose of diverse therapeutic strategies for CRS patients is to improve and restore their sinonasal MCC function, which in turn will reverse the pathological changes of diseased sinonasal mucosa (9, 31, 36).

The mucociliary apparatus consists of three functional components: the cilia on respiratory epithelium, the mucus layer, and the underlying airway surface liquid layer. How each of these three components is regulated and contributes to normal functioning of MCC is not entirely understood but is the subject of intense investigation. Recently, mice subjected to manipulation of genes encoding the components of the MCC apparatus have been generated (6, 7, 18, 21, 27, 39). In addition, a number of airway diseases, which usually present impaired MCC in humans, have also been modeled in mice by using genetic and pharmacological methodologies (7, 19, 21, 27, 41, 46, 47). Hence, these mouse models may become powerful tools to elucidate the molecular and mechanical mechanisms by which MCC is regulated and how impaired MCC contributes to the development of airway diseases.

Over the past several years, the mucociliary function in mouse lower airways and its regulatory mechanisms have been studied by using both in vitro and in vivo methodologies (12, 22). However, MCC function in the mouse nose has been less studied, and the methodologies to evaluate nasal MCC in vivo in mice are also more poorly developed. Although the MCC apparatus in the upper airways of mice has similar structure to that in the lower airways, their regulatory mechanisms are not identical. Mouse upper and lower airways have different profiles of ion channels responsible for water homeostasis, different mucin secretion mechanisms, different submucosal gland distributions and autonomic nerve systems (2, 3, 8, 12, 14, 16, 17, 40). Hence, development of reliable methodologies to conduct basic research on nasal MCC in mice is of great significance for our comprehensive understanding of MCC in the upper airways. It will also significantly advance our understanding of pathogenesis of inflammatory diseases in the upper airways such as chronic rhinosinusitis. In this study, we used planar gamma scintigraphy, a noninvasive methodology, to monitor the real-time nasal MCC rate in mice and defined its physiological features. We also compared the effect of differ-

* X. Hua and K. L. Zeman contributed equally to this study.

Address for reprint requests and other correspondence: X. Hua, CB 7219, Burnett Womack Bldg., Univ. of North Carolina at Chapel Hill, Chapel Hill, NC 27599 (e-mail: xiaoyang_hua@med.unc.edu).

ent breathing patterns, anesthetics, and inhaled saline aerosol perturbations on nasal MCC in mice. The development of this method will provide a useful tool to elucidate the molecular mechanisms by which the nasal MCC is regulated. It will also advance the studies on CRS pathogenesis and facilitate the development of new drugs for prospective treatment of CRS.

MATERIALS AND METHODS

Animals. All animal care and experimental procedures used were approved by the Institutional Animal Care and Use Committee guidelines of the University of North Carolina at Chapel Hill. C57BL/6 mice were originally purchased from the Jackson Laboratory and then housed and bred in a pathogen-free facility in the University of North Carolina at Chapel Hill, with 12:12-h day-night switch. All mice used in the study were 3- to 5-mo-old females. Food and water were allowed for all mice until the time of study.

A total of 40 mice were randomly divided into five groups, which were anesthetized with 1.1% isoflurane ($n = 14$), 2.1% isoflurane ($n = 6$), 3% isoflurane ($n = 6$), avertin (0.4 g/kg, $n = 8$), and pentobarbital (90 mg/kg, $n = 6$), respectively. The nasal MCC in each group was measured by scintigraphy for indicated periods of time immediately after the intranasal delivery of ^{99m}Tc-SC. In addition, another five and seven mice, which were both anesthetized by 1.1% isoflurane, were randomized to two groups and were treated with 0.9% saline and 10% saline aerosolization, respectively. The nasal MCC during and after the intervention in these two groups was also measured and compared with the nasal MCC in mice anesthetized with 1.1% isoflurane but without saline treatment.

Preparation of radiolabeled colloid. ^{99m}Technetium-labeled sulfur colloid particles (^{99m}Tc-SC) were prepared from TechneScan Sulfur Colloid Kits (CIS-Sulfur Colloid, CIS-US, Bedford, MA) following the procedure provided by the manufacturer. One microliter of 1% filtered Evan Blue dye was added to 30 μl of sulfur colloid suspension to aid in visualizing the liquid during application.

Nasal delivery of radioactivity particles. Mice were anesthetized with 5% isoflurane, which was delivered by an Ohio Vaporizer (DRE Veterinary). After successful anesthesia, 1 μl ^{99m}Tc-SC suspension in isotonic saline was slowly delivered into the mouse nose by using a PE-10 (Warner Instrument, OD 0.6 mm, ID 0.28 mm). For each mouse, the catheter was inserted into the nostril to a depth of 3 mm. For the mice that were anesthetized by either avertin (0.4 g/kg) or pentobarbital (90 mg/kg), ^{99m}Tc-SC was delivered in the same manner after successful anesthesia by intraperitoneal injection of these anesthetics. No isoflurane was used in these mice.

Whole nose acquisition by scintigraphy. After 1 μl ^{99m}Tc-SC was successfully delivered, mice were immediately placed supine on a level tray with the heads directly underneath a pinhole collimator associated with a planar gamma camera (Intel Medical). The mouse heads were covered with a transparent facial mask that connected with an isoflurane vaporizer. The upper incisors were slightly held with a U-shape metal wire inside the mask to better secure the mouse heads and to slightly overstretch the animal for optimal exposure of the mouse nose and nasopharynx (see Supplementary Fig. 1, *A* and *B*, available with the online version of this article). For those isoflurane-anesthetized mice, isoflurane was driven by filtered room air (0.7 l/min) and delivered into the facial mask with indicated concentrations; for those avertin- or pentobarbital-anesthetized mice, only filtered room air was delivered into the facial mask (0.7 l/min). To keep the distance between the mouse heads and the pinhole collimator constant, a spacer (2.5 cm) was used in all experiments. Mouse body temperature was maintained by using a heating pad. The images were then acquired by the gamma camera for indicated periods of time.

Determination of mouse nasal cavity and oropharynx in scintigraphic images. A preeuthanized mouse was immediately hung vertically by a rubber band that held the upper incisors. Mouse tongue was then pulled out to expose the oropharynx. A ^{99m}Tc-SC (1 μl) marker (round, ~2 mm in diameter) that was prewrapped with tape was carefully inserted into the mouse oropharynx. After that, 0.2 μl ^{99m}Tc-SC was carefully pipetted onto the tip of its external nose. This mouse was then put under the pinhole collimator at the same position as all other experimental animals. An image was acquired immediately.

Nasal mucociliary clearance rate interpretation. To quantify the MCC rate in the mouse nose, the whole nose retention of radioactivity by scintigraphy after ^{99m}Tc-SC nasal delivery was obtained for at least 1 h (1 min/frame). ImageJ (freeware from the National Institutes of Health) was used to analyze the data. Regions of interest were drawn around the nasal area. The radioactivity intensity (RI) was acquired every minute for indicated periods of time. From the second minute, the isotope decay correction was made.

Cumulative nasal MCC at every minute was calculated as the following formula: cumulative nasal MCC (%) = [(RI at T_{0min} minus RI)/RI at T_{0min}] × 100%. The nasal mucociliary clearance rate (% clearance per minute) was calculated as: mean of MCC = $\hat{\beta}_1 \times \text{time} + \hat{\beta}_2 \times \text{time}_{10}$ in Fig. 3, where $\hat{\beta}_1$ and $\hat{\beta}_2$ are the estimated parameter estimates for the two covariates time and time_{10} [$\text{time}_{10} = 0$ before 10 min; and $\text{time}_{10} = (\text{time} - 10)$ from 10 min forward]. Therefore, before 10 min, the nasal mucociliary clearance rate is estimated to be $\hat{\beta}_1$, and after 10 min, it is estimated to be $\hat{\beta}_1 - \hat{\beta}_2$. Similar approaches are used in other figures, except additional covariates are introduced.

Saline aerosol treatment. It is well known that hypertonic saline (HS) can enhance MCC in many species, including humans. To investigate whether or not HS has the same effect on nasal MCC in mice, we treated the mice with 1 ml 10% HS by aerosolization 4 min after ^{99m}Tc-SC intranasal delivery and monitored the cumulative nasal MCC for 60 min. Briefly, 1 ml saline at 10% was nebulized into a 50 ml conical tube by using AeroNeb (Aerogen, Ireland), which was placed upstream of the facial mask. Controls were treated with 0.9% saline. Saline aerosol together with isoflurane was driven through the conical tube by filtered room air (0.7 l/min) and delivered into the facial mask.

Statistical analysis. All analyses were conducted using SAS software (SAS, Cary, NC). The unit of randomization (to 5 anesthesia groups) and analysis in this study was the individual mouse. Since the end point of interest (retention rate) was measured repeatedly for each mouse within 60 min of acquisition, potential within-mice correlation of those repeated measures were considered. We used the generalized linear models for correlated data (i.e., mixed models) to assess the effects of anesthesia, treatment, or time on the retention rate. A compound symmetry or first-order autoregressive [AR(1)] covariance structure was assumed.

We first analyzed the subset of mice anesthetized with 1.1% isoflurane without other treatment to investigate the time course of radioactive particle clearance in the mouse nose. Only linear terms of time are our interest in this setting. We then evaluated the effect of different anesthetics on nasal MCC (avertin, pentobarbital intraperitoneal injection vs. 1.1% isoflurane inhalation). The anesthetics, time, and their interactions are included in the mixed model. Next, the analysis was conducted in the subset of mice anesthetized with 1.1%, 2.1%, and 3% isoflurane. In addition to the time and the isoflurane concentrations, breathing rates (BRs) of mice (at 0 minute, 30th minute, and 60th minute) were also considered as covariates in the mixed model. BRs of mice over time were also examined as an outcome across these groups. We finally analyzed the effect of hypertonic saline and isotonic saline on nasal MCC over time by including linear terms of time, treatment, and their interactions in the mixed model.

In this study, measurements are presented in the form of means ± SE.

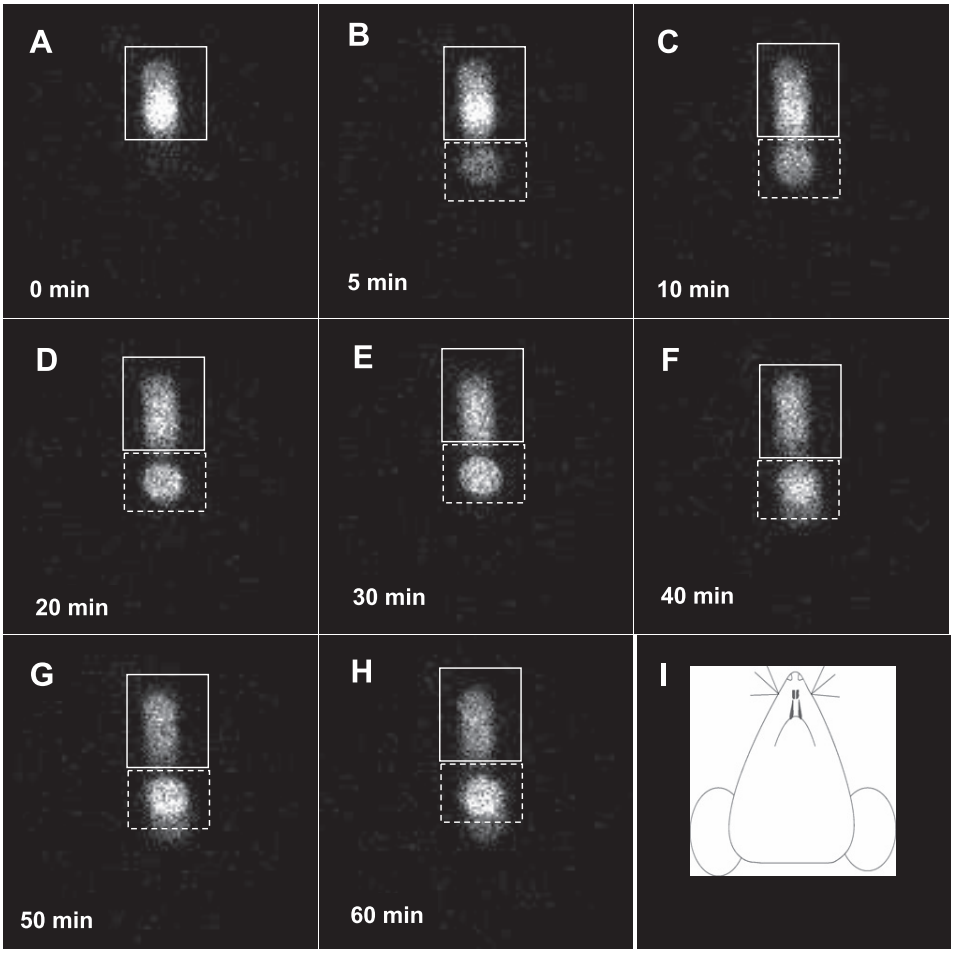

Fig. 1. Time course retention of radiolabeled particles in one representative mouse nose. After successful intranasal delivery of 1 μl ^{99m}technetium-labeled sulfur colloid (^{99m}Tc-SC) in normal saline, a mouse anesthetized by 1.1% isoflurane was placed supine under a pinhole collimator. The scintigraphic images were immediately acquired for 60 min (1 frame per minute). The images at 0, 5, 10, 20, 30, 40, 50, and 60 min were shown from *A* to *H*, respectively. The mouse head orientation in the images was schematically shown in *I*. The solid line squares indicated the initial ^{99m}Tc-SC deposition; those areas surrounded by dotted line squares indicated the newly formed deposition. The brightness of activity plaques represented the activity intensity, which reflected the radioisotopic counting rates.

RESULTS

Time course retention of radiolabeled particles in mouse nose. Representative images acquired by scintigraphy at 0, 5, 10, 20, 30, 40, 50, and 60 min are, respectively, presented in Fig. 1, *A–H*, after intranasal delivery of 1 μl ^{99m}technetium-sulfur colloid suspension in isotonic saline (^{99m}Tc-SC). As shown, the ^{99m}Tc-SC delivered to the nasal cavity initially formed one plaque (plaque A) in the image (Fig. 1*A*). These radioactive particles were subsequently moved caudally (see Supplementary Video I, available with the online version of this article). In ~5 min after the initial delivery, there was another activity plaque (plaque B) formed in the image (Fig. 1*B*), which was separated from the initial plaque A. These two activity plaques were constantly present in the images from 10 to 60 min (Fig. 1, *C–H*). Their relative locations in the images were not obviously altered, although their relative intensity changed significantly over time (Fig. 1, *B–H*). As shown, the radioactivity in plaque B of Fig. 1*B* was faded (5 min image), which was increased significantly from 10 to 60 min even with the presence of spontaneous isotope decay. In contrast, the intensity in plaque A was reduced significantly over time, suggesting that the particles originally placed at plaque A were continuously moved to and accumulated in plaque B. Collectively, according to these images and video, the nasal MCC function in live mice can be clearly visualized using the scintigraphic technique.

Identification of mouse nose in scintigraphic images. Figure 2*A* showed the markers, respectively, put at the tip of external nose and in the oropharynx of a euthanized mouse, which are clearly

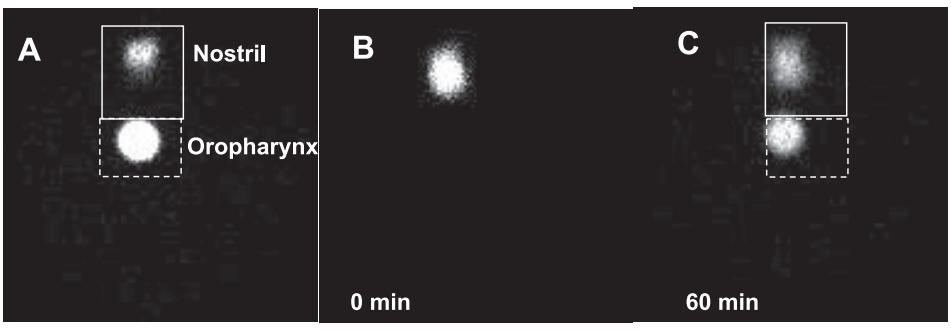

Fig. 2. Identification of mouse nose in scintigraphic images. *A*: the scintigraphic image showed the ^{99m}Tc-SC markers respectively placed in the oropharynx and external nose tip of a euthanized mouse. *B* and *C*: the scintigraphic images of one live mouse at 0 min (*B*) and 60 min (*C*) after intranasal delivery of 1 μl ^{99m}Tc-SC. The two mice used in both *A* and *B* were littermates, with matched age, sex, and body weight. Mouse heads were secured at the same position underneath the pinhole collimator during the acquisition.

presented in the scintigraphic image. In addition, a littermate of this mouse, which had been matched by sex and body weight, was used to acquire the images for 60 min after administration of 1 μl ^{99m}Tc-SC by intranasal delivery. As shown in Fig. 2*B*, one single radioactive plaque (Fig. 2*B*) at the very beginning (0 minute) was formed after intranasal ^{99m}Tc-SC delivery, which then formed two radioactive plaques similar to those described in Fig. 1 (Fig. 2*C*). When we compared the relative locations of plaques A and B in Fig. 2*C* to the radiomarkers in Fig. 2*A*, we observed that the marker showing the external nasal tip was more anterior to the location where the plaque A was in Fig. 2, *B* and *C*; and the marker put in the oropharynx showed the same location as the plaque B in Fig. 2*C*. Since each mouse's head was secured at the same place under the pinhole collimator, we conclude that plaque A and plaque B correspond to the nasal cavity and oropharynx in the images, respectively. In addition, in Supplementary Video II, we observed that the radioactive particles in plaque B were cleared by swallowing, further supporting that the anatomical location of plaque B was the oropharynx. These data indicate ^{99m}Tc-SC delivered into the mouse nasal cavity is subsequently cleared out of the nasal cavity and stored in the oropharynx, which is then cleared by swallowing.

Time course of radioactive particle clearance in the mouse nose. The 60-min cumulative nasal mucus clearance in the 1.1% isoflurane-anesthetized mice after ^{99m}Tc-SC delivery was 33.2% ± 4.23% (n = 14). As shown in Fig. 3*A*, the MCC rate in the nose can be divided into two phases: rapid phase, which is from 0–10 min, and slow phase, which is from 10 to 60 min. A piecewise linear regression of nasal mucus clearance on time with a break point at 10 min appears to fit the data well. Thus a mixed model with two covariates, time and $time_{10}$, is applied and an AR(1) within-mice correlation structure is assumed. Since the cumulative MCC at *time 0* is identically equal to 0, the regression was fitted without intercept. The P values for both predictors time and $time_{10}$ are <0.0001. Thus we reject the null hypothesis and conclude that both predictors are statistically significant. The corresponding parameter estimates suggest that the particles were cleared at a rate of 1.71% ± 0.17% of baseline level per minute from 0 to 10 min and 0.33% ± 0.06% per minute from 10 to 60 min (Fig. 3*B*). The predictor $time_{10}$ is also referred to as a linear spline term of time in this study.

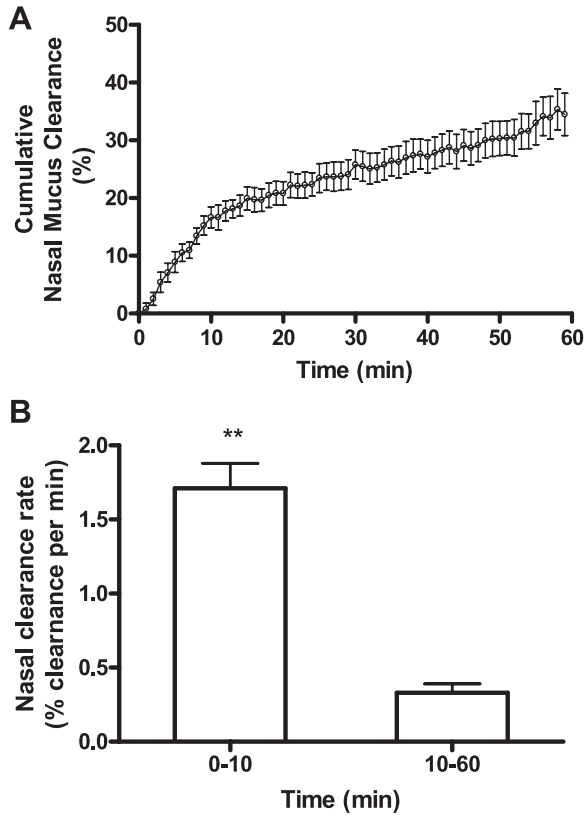

Fig. 3. Time course of radioactive particle clearance in the mouse nose. *A*: the nasal MCC in mice after intranasal delivery of 1 μl ^{99m}Tc-SC (n = 14). Data represent the mean cumulative nasal mucus clearance ± SE, presented as % clearance. *B*: the nasal mucociliary clearance (MCC) rate from 0–10 min and from 10–60 min. Data represent the mean nasal MCC rate ± SE, presented as % clearance per minute. **P < 0.001.

Effect of anesthetics on nasal MCC. Anesthesia has long been observed to have inhibitory effects on MCC in humans and other species (13, 20, 23). In this project to measure nasal MCC by scintigraphy, anesthesia is also needed to immobilize the mice under the gamma camera. To select an appropriate anesthetic that has the least effect on MCC, three different anesthetics, avertin (0.4 g/kg ip), pentobarbital (90 mg/kg ip), and the gas isoflurane (1.1% vol/vol), were used. The effect of these anesthetics on nasal MCC measured by scintigraphy was compared. First, all three different anesthesia methods can effectively immobilize the animals without causing mortality during the experiments. Second, by using all three different anesthesia methods, all mice can breathe evenly without active sniffing or sneezing. Since the avertin effect only lasts 30–50 min, we only measured the MCC for 30 min following administration of anesthesia and particle delivery. As shown in Fig. 4, both avertin (at 0.4 g/kg) and pentobarbital (at 90 mg/kg) significantly inhibited the nasal MCC compared with 1.1% isoflurane (Fig. 4*A*). Based on the data analysis results in Fig. 3, we applied a mixed model with covariates time, $time_{10}$, anesthesia, interaction between time and anesthesia, and between $time_{10}$ and anesthesia, assuming an AR(1) covariance structure. The results suggest that there is no significant difference between pentobarbital and avertin anesthetized groups (P > 0.05 if we test the avertin, avertin × time, and avertin × $time_{10}$ jointly with pentobarbital as the reference). Therefore, we pooled the mice with pentobarbital and avertin together and conduct the same analysis again. Between 1.1% isoflurane and the other two groups, both interactions of anesthesia and time, and anesthesia and $time_{10}$ are significant with P values < 0.0001. That is, the pattern of change in nasal MCC over time (0–30 min) is statistically different between 1.1% isoflurane and the other two groups. Before 10 min, the nasal MCC is expected to increase 1.68% ± 0.18% of baseline level per minute for isoflurane group; however, only 0.19% ± 0.18% per minute were expected in the other two groups. Between 10–30 min, the nasal MCC slows down, only 0.39% ± 0.12% per minute for the 1.1% isoflurane group, and 0.55% ± 0.12% per minute for the other two groups (Fig. 4*B*). Hence, these data indicate that isoflurane at 1.1% effectively immobilizes the mice and has the least effect on nasal MCC during the scintigraphic acquisition.

Dose response of isoflurane on nasal MCC. To further investigate the effect of isoflurane on nasal MCC in mice, the dose response of this anesthetic was examined. As shown in

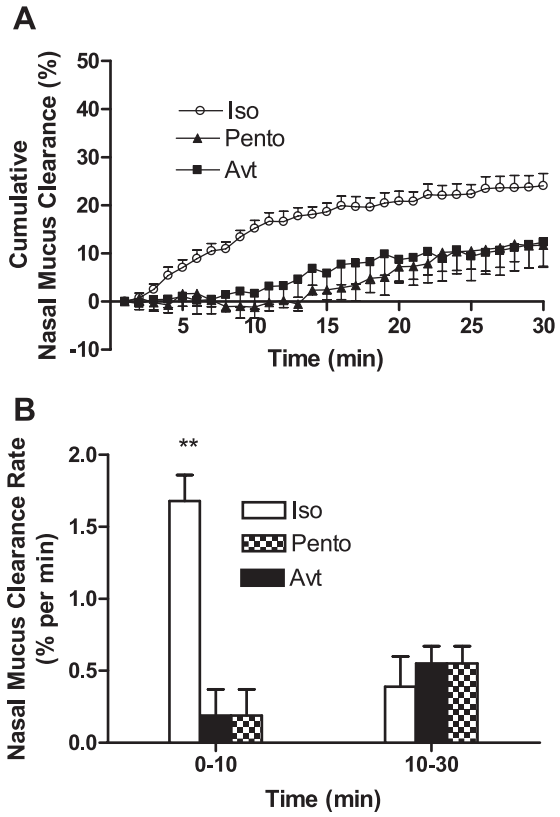

Fig. 4. Effect of pentobarbital and avertin on nasal MCC. *A*: the cumulative nasal MCC in mice anesthetized by pentobarbital (Pento, 90 mg/kg, ▲, $n = 6$) and avertin (Avt, 0.4 g/kg, ■, $n = 8$). ○, cumulative nasal MCC in mice anesthetized by 1.1% isoflurane (Iso, $n = 14$). Data represent the mean cumulative nasal MCC ± SE, presented as % clearance. $P < 0.0001$, both avertin and pentobarbital groups vs. 1.1% isoflurane anesthetized group; $P > 0.05$ between avertin and pentobarbital groups. *B*: the nasal MCC rate from 0–10 min and from 10–30 min in mice anesthetized with avertin, pentobarbital, and 1.1% isoflurane. Data represent the mean nasal MCC rate ± SE, presented as % clearance per minute. $^{**}P < 0.001$.

Fig. 5*A*, the nasal MCC in mice anesthetized with 2.1% and 3% isoflurane have similar patterns over time as the 1.1% isoflurane-treated group. There is no obvious break point in time in MCC over time. Thus a mixed model with covariates treatment and time (no interaction) would be appropriate. In addition, we also recorded the breath rates of these mice to evaluate the depth of anesthesia at these three different isoflurane concentrations. As shown in Fig. 5*B*, when the isoflurane concentration was set at 1.1%, the BRs of mice were, respectively, 105.6 ± 1.8, 93.3 ± 3.5, and 87.7 ± 2 breaths/min at 0, 30 and 60 min. However, when the concentration of isoflurane was increased to 2.1% and 3%, the BRs of mice were significantly decreased. The BRs of mice anesthetized with 2.1% isoflurane were 37.5 ± 1.8, 30 ± 0.89, and 23 ± 4.6 breaths/min at 0, 30 and 60 min; those in 3% isoflurane-anesthetized group were 28.3 ± 0.52, 22 ± 3.7, and 0 ± 0 breaths/min, respectively. In a mixed model for BRs and using time, isoflurane groups and their interactions as predictors, there is significant difference in BRs between the groups over time ($P < 0.0001$ for 4 degrees of freedom if testing isoflurane and time-isoflurane interactions jointly). Hence, although isoflurane concentration increases from 1.1% to 3% producing anesthesia with depth ranging from very light to very deep (lethal), the nasal MCC rates were not significantly changed. These data not only suggest a smaller effect of isoflurane vs. other anesthetics used in this study on nasal MCC in mice, but also indicate that the range of isoflurane concentration that can be applied for nasal MCC measurement is very wide.

In a mixed model with retention rate at 0, 30, and 60 min as outcomes, time, treatment, and BRs as predictors, and assuming compound symmetry covariance structure, there is no significant treatment effect ($P = 0.81$). In addition, we also failed to observe a significant effect of breathing pattern change on the particle clearance ($P = 0.97$). Change from a faster and shallow breathing pattern to a slow and deeper one, which was induced by the administration of isoflurane at different concentrations in this study, failed to alter the nasal MCC in mice. Hence, these data also indicate that significant change in breathing pattern does not change nasal MCC in mice.

Effect of hypertonic saline and isotonic saline on nasal MCC. The effects of HS and isotonic saline on nasal MCC were also examined. As shown in Fig. 6, HS treatment immediately enhanced the nasal MCC. The (0–60 min) cumulative nasal MCC in the HS-treated group was increased significantly, with the rate slowing after 10 min and further after 20 min. Therefore, a mixed model with covariates time, $time_{10}$, $time_{20}$, treatment, time-treatment, and $time_{20}$-treatment inter-

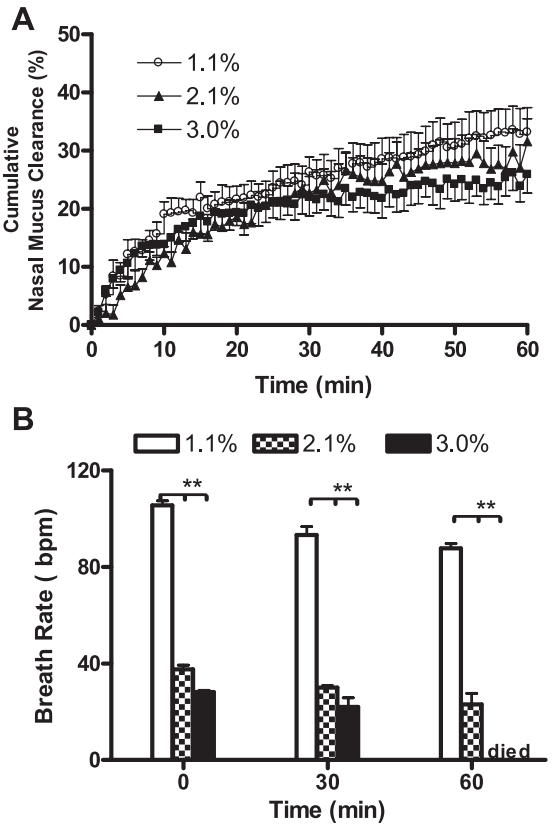

Fig. 5. Dose response of isoflurane on nasal MCC and breathing rate in mice. *A*: the cumulative nasal MCC in 1.1% ($n = 7$, ○), 2.1% ($n = 6$, ▲), and 3% ($n = 6$, ■) isoflurane-anesthetized mice. Data represent the mean nasal MCC ± SE, presented as % clearance. $P > 0.05$ between each two of the three groups. *B*: the mean breathing rates (BRs) of these three groups at indicated time point. Data represent the mean BRs ± SE. $^{**}P < 0.001$, 1.1% vs. both 2.1% and 3% isoflurane-anesthetized mice. bpm, breaths/min.

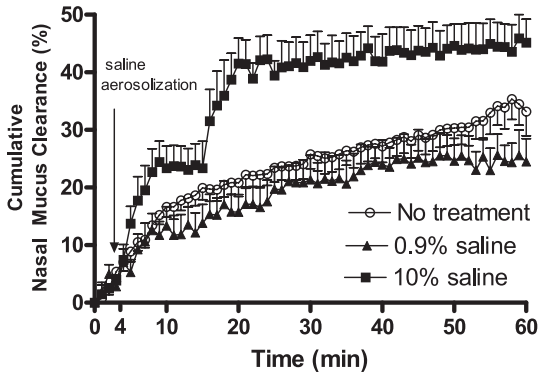

Fig. 6. Effect of hypertonic saline on nasal MCC in mice. Cumulative nasal MCC in mice treated with isotonic saline (0.9%, ▲, $n = 5$) or hypertonic saline (10%, ■, $n = 7$). Controls were mice subjected to the same anesthesia without any treatment ($n = 14$, ○). Data represent the mean cumulative nasal MCC ± SE, presented as % clearance. $P > 0.05$ between isotonic saline and control groups; $P < 0.001$ between hypertonic saline and control groups.

actions are fitted ($P < 0.001$ for both time-treatment, and $time_{20}$-treatment interactions). In addition, the pattern of change is significantly different between HS-treated group and the controls. Before 10 min, MCC increased at a much faster rate with HS treatment, but after that, the control group matched the HS-treated group with MCC in both groups slowing down significantly. In addition, we also noticed that the difference between these two groups was reduced over time. There is no statistical difference between these groups post-54 min (Fig. 6, $P > 0.05$). We also treated the mice with isotonic saline to rule out the possibility that the observed HS effect on MCC was a result of airway humidification. As shown, isotonic saline did not significantly change the nasal MCC in mice.

DISCUSSION

In this report, we have presented an in vivo method to measure the real-time nasal MCC rate of mice by using gamma scintigraphy. We also compare the effect of different anesthetics on nasal MCC and define the physiological features of nasal MCC of mice. We found that 1.1% isoflurane inhalation had the least inhibitory effect on nasal MCC compared with avertin and pentobarbital, two other anesthetics that have been frequently used in animal experiments. In addition, increasing doses of isoflurane have no significant effect on nasal MCC. In mice lightly anesthetized by isoflurane, the nasal MCC exhibits two distinct phases: rapid phase and slow phase. HS, which has long been observed capable of speeding up the airway MCC escalator in humans and other species, can also significantly accelerate the nasal MCC of mice. In addition, we have also compared the effect of different breathing patterns on nasal MCC and conclude that in isoflurane-anesthetized mice, the MCC escalator is the major mechanism by which predelivered particles are cleansed from the surface of the mouse nose.

To the best of our knowledge, this is the first report of in vivo measurement of nasal MCC rate in live laboratory mice. The advantages of this method include *1*) nasal MCC of mice can be monitored in a real-time manner; *2*) this methodology is noninvasive, and the ^{99m}Tc-SC in the mouse nose can be cleared in 2–3 days by both MCC and decay; therefore, the animals may be reused for crossover studies (e.g., testing new therapies), which will also reduce the animal numbers and the related costs for a given project; *3*) the nasal MCC is measured under a condition very close to the actual physiological conditions; *4*) drugs or other medical interventions can be given during the nasal MCC measurement to observe their immediate effect on nasal MCC; and *5*) it provides a measure of the comprehensive function of the mucociliary apparatus in mouse nose rather than assessing the function of one single component.

MCC is a very complex process. Impairment of each of the three components of the MCC apparatus, cilia beating, mucus secretion, and water homeostasis in the airway lumen, will lead to dysfunction of MCC. Over the past decades, a number of methodologies have been developed for nasal MCC studies in mice at both in vivo and in vitro levels, including microdialysis probes, visualized MCC hurricane on airway epithelial cultures, and recording of cilia beating frequency (1, 15, 29). The in vitro methodologies using either explants or cultured cells do not necessarily represent the MCC functions in vivo in which autonomic nervous and neuroendocrine systems are intact (1). Recording of cilia beating frequency will only assess the function of cilia and is not informative in terms of other factors that are involved in normal functioning of nasal MCC such as the mucus rheology in the nose (1). The microdialysis probe is a recently reported method to measure nasal MCC in vivo. Grubb et al. (15) used a microdialysis probe positioned at the mouse nasopharynx to detect the presence of rhodamine dye, which was preloaded to mouse nasal cavity, in mouse nasopharyngeal preparation. The distance between where the dye was deposited in mouse nose and the tip of microdialysis probe was also measured. The in vivo MCC transport was calculated by dividing this distance with the elapsed time from the deposition to the detection of dye by microdialysis probe. This technique elegantly defined MCC velocity in vivo although it is still invasive. Moreover, by using this method, the time course for mucus clearance in mouse nose cannot be defined. We believe that the capacity to measure the time course of MCC afforded by whole nose acquisition using gamma scintigraphy will be an important complement to developed methodologies for nasal MCC studies and will provide more comprehensive information about mucus clearance in the nose and sinuses.

Although the MCC apparatus in the upper and lower airways has similar structure, quite a few reports have recently suggested that their regulatory mechanisms are different. For example, the respiratory epithelial cells in mouse upper and lower airways may have different ion channel profiles that are responsible for water homeostasis in the airway lumen (14, 16, 17); the mucus secretion mechanisms and the innervation of mouse upper and lower airways are also different (2, 3, 12). Hence, development of this methodology to measure nasal MCC in vivo will help our understanding of the role of MCC in the upper airway and the pathogenesis of upper airway diseases such as chronic rhinosinusitis.

By using gamma scintigraphy, we observed that nasal MCC of isoflurane-anesthetized mice has two distinct phases: the rapid phase and the slow phase. The overall clearance rates during these two phases are 1.71% and 0.33% per minute, respectively, which are significantly different. This is very similar to the MCC in the lungs and lower airways of several species including humans (10, 12, 24). In the lungs and lower airways, the rapid phase is thought to represent the clearance in the central airways, whereas the slow phase is believed to repre-

sent that in the small airways and alveoli (12, 24). The mechanisms of clearance in the lungs and airways during these two phases are also different. The clearance during the rapid phase is mainly driven by MCC escalator, whereas the clearance during the slow phase is mainly achieved by macrophage engulfment with the involvement of mucociliary escalator during the early period of this phase (10, 12, 24, 33). However, for the nasal MCC in mice, it is not clear what the rapid and slow phases represent and the underlying mechanisms by which the clearance is achieved during these two phases. Grubb et al. (15) reported that the mucociliary transport rate (MCT) in different anatomical sites in the murine nose was significantly different. This regional difference is mainly due to the different rheology of the mucus blanket in different anatomical sites since the cilia beating frequency of nasal epithelial cells in different regional sites has been reported to be very uniform (4, 37). Hence, it is likely that the two distinct phases observed in our study reflect the regional difference in MCT in the mouse nose. The second explanation in this regard is the likely deposition of ^{99m}Tc-SC particles on nonrespiratory epithelium in mouse nose. The rodent nose is different from humans in both anatomy and histology. More than 50% of the nasal cavity surface of rodents is lined by olfactory epithelium (44). Hence, it is likely that a fair amount of the ^{99m}Tc-SC particles delivered into the mouse nose will be deposited on olfactory epithelial cells initially. The olfactory epithelium does not contain cilia. Hence particles deposited onto olfactory epithelium need to be moved to respiratory epithelium by some other mechanisms to become clearable, i.e., represented by the slow phase in our nasal MCC data. This also suggests that the initial distribution of radiolabeled particles in the mouse nose is an important factor that determines the nasal MCC rate measured by scintigraphy. In this study, we strictly employed the same method to deliver ^{99m}Tc-SC particles in each mouse; hence, we assumed that the initial deposition of ^{99m}Tc-SC particles was identical, which was also supported by the high reproducibility of our data.

In this report, we also compared the inhibitory effect of different anesthetics on nasal MCC. We found that both avertin (0.4 g/kg) and pentobarbital (90 mg/kg) can significantly inhibit the nasal MCC in mice. They mainly inhibited the rapid phase of MCC in mouse noses. The inhibitory effect of barbiturates on MCC has long been reported in other species including dogs, sheep, and rats (5, 23, 34). Our data show a potent inhibitory effect of both pentobarbital and avertin on nasal MCC in mice. Hence, these data suggest that for measurement of MCC in the mouse nose, both avertin and pentobarbital should be avoided.

In contrast to pentobarbital and avertin, we found that lower concentration of isoflurane (1.1%) could effectively immobilize the animals and had much less effect on nasal MCC. This was further supported by the dose response of isoflurane. Isoflurane at 2.1% and 3% could anesthetize mice very deeply (breathing rate was significantly inhibited; isoflurane at 3% was lethal in all tested mice in 30–60 min), although the nasal MCC rates in mice anesthetized by 2.1% and 3% isoflurane were not statistically different from that in 1.1% isoflurane-anesthetized animals. Isoflurane is a very commonly used volatile anesthetic in humans. It has long been suggested that volatile anesthetics including isoflurane can elicit depression of airway clearance (25, 30). Hence, physicians have always been concerned that using volatile anesthetics may increase the incidence of postoperative airway infections. In rabbits, Tyrakowski et al. (38, 42) found that very high concentration of isoflurane dissolved in Ringer buffer can abolish mechanical stimulation-induced transepithelial potential difference (PD) hyperpolarization reactions in excised rabbit tracheal epithelium. However, at lower concentrations, which are more clinically relevant, isoflurane has no such effect. In this report, we also found that isoflurane at concentration $<2\%$ has a very small effect on nasal MCC; however, there was a trend of impaired nasal MCC in 3% isoflurane-anesthetized mice. Hence, these studies further suggest that the effect of isoflurane on MCC may be dose dependent and that low concentrations of isoflurane may have a less significant inhibitory effect on MCC.

Hypertonic saline has long been observed capable of speeding up airway MCC in humans (10). It has also been used to treat a number of airway diseases with impaired MCC, such as cystic fibrosis (10, 11). In this report, we also found that hypertonic saline could significantly accelerate nasal MCC in a pattern very similar to that reported in human studies. Daviskas et al. (10) reported that hypertonic saline treatment could immediately enhance the MCC in the lungs and lower airways of healthy adult humans; the effect of hypertonic saline lasted for ~20 min until the emergence of slow phase. In our study, the nasal MCC was sped up 2–3 min after the hypertonic saline treatment, which lasted for about 15–18 min until the emergence of the slow phase.

Conclusion. In this report, we have demonstrated a novel in vivo method to measure the real-time nasal MCC rate in live laboratory mice. By using gamma scintigraphy techniques, we have defined two successive physiological phases of nasal MCC in mice and compared the effect of different anesthetics on nasal MCC. Due to the availability of mouse models with modifications of genes closely associated with abnormal MCC function, this technique will allow investigators to carry out more sophisticated studies to elucidate mechanisms by which the nasal MCC is regulated and to define the pathogenesis of many human upper airway diseases with impaired nasal MCC. It will also significantly facilitate the discovery of novel drugs to improve nasal MCC function and test the impact of intranasal drugs on MCC function in both diseased and normal conditions.

ACKNOWLEDGMENTS

We thank the Keck family for generous support of the Keck Animal Models Facility at the University of North Carolina, Dr. Brian Button for providing technical support, Dr. Jihong Wu for preparing the 99m-technetium-sulfur colloid solution, and Warren C. Naselsky and Richard J. Norris for reviewing the manuscript.

GRANTS

This work was supported by Cystic Fibrosis Foundation Grant BUTTON07XX0 to W. D. Bennett and Dr. Button, AAO-HNS/AAOA Core Grant 92997 to X. Hua, the Chinese National Natural Science Foundation Grant 30700933 to X. Hua, National Institute of Allergy and Infectious Diseases Grant U19AI077437 to D. B. Peden, and National Heart, Lung, and Blood Institute Grant HL-071802-05 A1 to S. L. Tilley.

DISCLOSURES

No conflicts of interest are declared by the authors.

REFERENCES

1. **Antunes MB, Cohen NA.** Mucociliary clearance—a critical upper airway host defense mechanism and methods of assessment. *Current Opin Allergy Clin Immunol* 7: 5–10, 2007.
2. **Baraniuk JN.** Neural regulation of mucosal function. *Pulm Pharmacol Ther* 21: 442–448, 2008.
3. **Belvisi MG.** Overview of the innervation of the lung. *Current Opin Pharmacol* 2: 211–215, 2002.
4. **Braverman I, Wright ED, Wang CG, Eidelman D, Frenkiel S.** Human nasal ciliary-beat frequency in normal and chronic sinusitis subjects. *J Otolaryngol* 27: 145–152, 1998.
5. **Bridger GP, Proctor DF.** Mucociliary function in the dog's larynx and trachea. *Laryngoscope* 82: 218–224, 1972.
6. **Brody SL, Yan XH, Wuerffel MK, Song SK, Shapiro SD.** Ciliogenesis and left-right axis defects in forkhead factor HFH-4-null mice. *Am J Respir Cell Mol Biol* 23: 45–51, 2000.
7. **Chen J, Knowles HJ, Hebert JL, Hackett BP.** Mutation of the mouse hepatocyte nuclear factor/forkhead homologue 4 gene results in an absence of cilia and random left-right asymmetry. *J Clin Invest* 102: 1077–1082, 1998.
8. **Clarke LL, Grubb BR, Yankaskas JR, Cotton CU, McKenzie A, Boucher RC.** Relationship of a non-cystic fibrosis transmembrane conductance regulator-mediated chloride conductance to organ-level disease in Cftr(−/−) mice. *Proc Natl Acad Sci USA* 91: 479–483, 1994.
9. **Cohen NA.** Sinonasal mucociliary clearance in health and disease. *Ann Otol Rhinol Laryngol* 196: 20–26, 2006.
10. **Daviskas E, Anderson SD, Gonda I, Eberl S, Meikle S, Seale JP, Bautovich G.** Inhalation of hypertonic saline aerosol enhances mucociliary clearance in asthmatic and healthy subjects. *Eur Respir J* 9: 725–732, 1996.
11. **Donaldson SH, Bennett WD, Zeman KL, Knowles MR, Tarran R, Boucher RC.** Mucus clearance and lung function in cystic fibrosis with hypertonic saline. *N Engl J Med* 354: 241–250, 2006.
12. **Foster WM, Walters DM, Longphre M, Macri K, Miller LM.** Methodology for the measurement of mucociliary function in the mouse by scintigraphy. *J Appl Physiol* 90: 1111–1117, 2001.
13. **Gosselink R, Gayan-Ramirez G, Houtmeyers E, de Paepe K, Decramer M.** High-dose lidocaine reduces airway mucus transport velocity in intubated anesthetized dogs. *Respir Med* 100: 258–263, 2006.
14. **Grubb BR, Boucher RC.** Pathophysiology of gene-targeted mouse models for cystic fibrosis. *Physiol Rev* 79: S193–214, 1999.
15. **Grubb BR, Jones JH, Boucher RC.** Mucociliary transport determined by in vivo microdialysis in the airways of normal and CF mice. *Am J Physiol Lung Cell Mol Physiol* 286: L588–L595, 2004.
16. **Grubb BR, Paradiso AM, Boucher RC.** Anomalies in ion transport in CF mouse tracheal epithelium. *Am J Physiol Cell Physiol* 267: C293–C300, 1994.
17. **Grubb BR, Vick RN, Boucher RC.** Hyperabsorption of Na^+ and raised Ca^{2+}-mediated Cl^- secretion in nasal epithelia of CF mice. *Am J Physiol Cell Physiol* 266: C1478–C1483, 1994.
18. **Ibanez-Tallon I, Gorokhova S, Heintz N.** Loss of function of axonemal dynein Mdnah5 causes primary ciliary dyskinesia and hydrocephalus. *Hum Mol Genet* 11: 715–721, 2002.
19. **Jacob A, Faddis BT, Chole RA.** Chronic bacterial rhinosinusitis: description of a mouse model. *Arch Otolaryngol Head Neck Surg* 127: 657–664, 2001.
20. **Kesimci E, Bercin S, Kutluhan A, Ural A, Yamanturk B, Kanbak O.** Volatile anesthetics and mucociliary clearance. *Minerva Anestesiol* 74: 107–111, 2008.
21. **Kobayashi Y, Watanabe M, Okada Y, Sawa H, Takai H, Nakanishi M, Kawase Y, Suzuki H, Nagashima K, Ikeda K, Motoyama N.** Hydrocephalus, situs inversus, chronic sinusitis, and male infertility in DNA polymerase lambda-deficient mice: possible implication for the pathogenesis of immotile cilia syndrome. *Mol Cell Biol* 22: 2769–2776, 2002.
22. **Kurosawa H, Wang CG, Dandurand RJ, King M, Eidelman DH.** Mucociliary function in the mouse measured in explanted lung tissue. *J Appl Physiol* 79: 41–46, 1995.
23. **Landa JF, Hirsch JA, Lebeaux MI.** Effects of topical and general anesthetic agents on tracheal mucous velocity of sheep. *J Appl Physiol* 38: 946–948, 1975.
24. **Langenback EG, Bergofsky EH, Halpern JG, Foster WM.** Determining deposition sites of inhaled lung particles and their effect on clearance. *J Appl Physiol* 68: 1427–1434, 1990.
25. **Lee KS, Park SS.** Effect of halothane, enflurane, and nitrous oxide on tracheal ciliary activity in vitro. *Anesthesia Analgesia* 59: 426–430, 1980.
26. **Lee L, Campagna DR, Pinkus JL, Mulhern H, Wyatt TA, Sisson JH, Pavlik JA, Pinkus GS, Fleming MD.** Primary ciliary dyskinesia in mice lacking the novel ciliary protein Pcdp1. *Mol Cell Biol* 28: 949–957, 2008.
27. **Mall M, Grubb BR, Harkema JR, O'Neal WK, Boucher RC.** Increased airway epithelial Na^+ absorption produces cystic fibrosis-like lung disease in mice. *Nature Med* 10: 487–493, 2004.
28. **Mall MA.** Role of cilia, mucus, and airway surface liquid in mucociliary dysfunction: lessons from mouse models. *J Aerosol Med Pulmonary Drug Deliv* 21: 13–24, 2008.
29. **Matsui H, Randell SH, Peretti SW, Davis CW, Boucher RC.** Coordinated clearance of periciliary liquid and mucus from airway surfaces. *J Clin Invest* 102: 1125–1131, 1998.
30. **Matsuura S, Shirakami G, Iida H, Tanimoto K, Fukuda K.** The effect of sevoflurane on ciliary motility in rat cultured tracheal epithelial cells: a comparison with isoflurane and halothane. *Anesthesia Analgesia* 102: 1703–1708, 2006.
31. **Meltzer EO, Hamilos DL, Hadley JA, Lanza DC, Marple BF, Nicklas RA, Bachert C, Baraniuk J, Baroody FM, Benninger MS, Brook I, Chowdhury BA, Druce HM, Durham S, Ferguson B, Gwaltney JM Jr, Kaliner M, Kennedy DW, Lund V, Naclerio R, Pawankar R, Piccirillo JF, Rohane P, Simon R, Slavin RG, Togias A, Wald ER, Zinreich SJ.** Rhinosinusitis: Establishing definitions for clinical research and patient care. *Otolaryngol Head Neck Surg* 131: S1–S62, 2004.
32. **Noone PG, Leigh MW, Sannuti A, Minnix SL, Carson JL, Hazucha M, Zariwala MA, Knowles MR.** Primary ciliary dyskinesia: diagnostic and phenotypic features. *Am J Respir Crit Care Med* 169: 459–467, 2004.
33. **Oberdorster G, Cox C, Gelein R.** Intratracheal instillation versus intratracheal-inhalation of tracer particles for measuring lung clearance function. *Exp Lung Res* 23: 17–34, 1997.
34. **Patrick G, Stirling C.** Measurement of mucociliary clearance from the trachea of conscious and anesthetized rats. *J Appl Physiol* 42: 451–455, 1977.
35. **Pleis JR, Lethbridge-Cejku M.** Summary health statistics for U.S. adults: National Health Interview Survey, 2006. *Vital Health Stat*: 1–153, 2007.
36. **Senior BA, Kennedy DW, Tanabodee J, Kroger H, Hassab M, Lanza D.** Long-term results of functional endoscopic sinus surgery. *Laryngoscope* 108: 151–157, 1998.
37. **Shaari J, Palmer JN, Chiu AG, Judy KD, Cohen AS, Kennedy DW, Cohen NA.** Regional analysis of sinonasal ciliary beat frequency. *Am J Rhinol* 20: 150–154, 2006.
38. **Smuszkiewicz P, Drobnik L, Mieszkowski J, Konikowski A, Holynska I, Kaczorowski P, Tyrakowski T.** Comparison of the influence of halothane and isoflurane on airway transepithelial potential difference. *Pharmacol Rep* 58: 736–745, 2006.
39. **Snouwaert JN, Brigman KK, Latour AM, Malouf NN, Boucher RC, Smithies O, Koller BH.** An animal model for cystic fibrosis made by gene targeting. *Science* 257: 1083–1088, 1992.
40. **Tarran R, Grubb BR, Parsons D, Picher M, Hirsh AJ, Davis CW, Boucher RC.** The CF salt controversy: in vivo observations and therapeutic approaches. *Molec Cell* 8: 149–158, 2001.
41. **Temann UA, Geba GP, Rankin JA, Flavell RA.** Expression of interleukin 9 in the lungs of transgenic mice causes airway inflammation, mast cell hyperplasia, and bronchial hyperresponsiveness. *J Exp Med* 188: 1307–1320, 1998.
42. **Tyrakowski T, Smuszkiewicz P, Drobnik L, Marzec M, Mlodzik-Danielewicz N, Lelinska A, Kaczorowski P.** Effects of halothane and isoflurane on stimulated airway transepithelial ion transport. *Pharmacol Rep* 57: 550–555, 2005.
43. **van der Baan B.** Ciliary function. *Acta Otorhinolaryngol Belg* 54: 293–298, 2000.
44. **Wagner JG, Harkema JR.** Rodent models of allergic rhinitis: relevance to human pathophysiology. *Current Allergy Asthma Rep* 7: 134–140, 2007.
45. **Xu BP, Shen KL, Hu YH, Feng XL, Li HM, Lang ZQ.** [Clinical characteristics of primary ciliary dyskinesia in children]. *Zhonghua er ke za zhi* 46: 618–622, 2008.
46. **Yu M, Tsai M, Tam SY, Jones C, Zehnder J, Galli SJ.** Mast cells can promote the development of multiple features of chronic asthma in mice. *J Clin Invest* 116: 1633–1641, 2006.
47. **Zhu Z, Homer RJ, Wang Z, Chen Q, Geba GP, Wang J, Zhang Y, Elias JA.** Pulmonary expression of interleukin-13 causes inflammation, mucus hypersecretion, subepithelial fibrosis, physiologic abnormalities, and eotaxin production. *J Clin Invest* 103: 779–788, 1999.